Dimensional Crossover of the Integer Quantum Hall Plateau Transition and Disordered Topological Pumping

Matteo Ippoliti[1] and R. N. Bhatt[2]
[1]Department of Physics, Princeton University, Princeton, New Jersey 08544, USA
[2]Department of Electrical Engineering, Princeton University, Princeton, New Jersey 08544, USA

(Received 5 June 2019; accepted 11 February 2020; published 27 February 2020)

We study the quantum Hall plateau transition on rectangular tori. As the aspect ratio of the torus is increased, the two-dimensional critical behavior, characterized by a subthermodynamic number of topological states in a vanishing energy window around a critical energy, changes drastically. In the thin-torus limit, the entire spectrum is Anderson localized; however, an *extensive* number of states retain a Chern number $C \neq 0$. We resolve this apparent paradox by mapping the thin-torus quantum Hall system onto a disordered Thouless pump, where the Chern number corresponds to the winding number of an electron's path in real space during a pump cycle. We then characterize quantitatively the crossover between the one- and two-dimensional regimes for finite torus thickness, where the average Thouless conductance also shows anomalous scaling.

DOI: 10.1103/PhysRevLett.124.086602

Introduction.—The integer quantum Hall plateau transition [1] has a long and rich history as an example of the interplay between disorder and topology in condensed matter. While the quantization is ultimately due to the presence of a topological invariant [2,3], its astonishing precision is due to disorder-induced localization of electron states away from the critical energy [4]. In a high magnetic field, the motion of electrons is confined to the lowest Landau level (LLL). The LLL carries a nonzero Chern number, a topological invariant related to the Hall conductance, which forbids complete localization of the spectrum. A critical energy exists where the electron localization length ξ diverges, explaining the plateau transition as a quantum critical point that has successfully been studied by means of scaling theories [5]. However, the precise value of ν, the critical exponent characterizing the divergence of ξ, and whether or not it agrees with experiment [6–9], remains controversial [10–12].

Most numerical studies of the critical exponent have relied on the transfer matrix method for either the original continuum LLL problem [13,14] or the Chalker-Coddington network model [15–18] on strip geometries. On the other hand, purely two-dimensional methods to determine ν have been developed based on the topological character of individual eigenstates [19,20] (an idea that has since been used in several studies [11,21–27]), the disorder-averaged Hall [28,29], Thouless [29,30] and longitudinal [31] conductance, as well as quantum diffusion [32]. Here one considers a square torus with both sides scaled concurrently, $L_x = L_y \sim N_\phi^{1/2}$ (N_ϕ is the number of magnetic flux quanta through the system, proportional to the system's area). The number of states with nonzero Chern number (hereafter simply called Chern states) is found to diverge subextensively with system size, as $N_\phi^{1-(1/2\nu)}$ [19]. The success of methods based on the Chern number in square geometry motivates their application to rectangular geometries $L_x > L_y$ with varying aspect ratio $a = L_x/L_y$, and particularly in the quasi-one-dimensional limit $a \to \infty$ at fixed thickness, reminiscent of the transfer matrix calculations. This is especially interesting because the defining feature of the 2D problem (the presence of a topologically robust Hall conductance, encoded in the Chern number C) does not have an obvious one-dimensional counterpart. While the mathematical definition of C holds regardless of system size or aspect ratio, on physical grounds the system in the quasi-1D limit must be described by a local, disordered free-fermion chain—essentially the Anderson model [33]. This raises the question of what happens to Chern states in this limit, and how the topological character of the LLL is manifested once the system is mapped onto a 1D Anderson insulator.

One may reasonably expect, given the stronger tendency towards localization in one-dimensional systems [34], that quasi-1D scaling will lead to a faster decay of the fraction of Chern states relative to the 2D case (where the fraction falls off as $N_\phi^{-(1/2\nu)}$), perhaps even to saturate the lower bound N_ϕ^{-1} (achieved if all states but one have $C = 0$). In fact, we find quite the opposite: Chern states do *not* vanish under 1D scaling. On the contrary, they represent a finite fraction of all states—and asymptotically take over the entire spectrum.

As a byproduct, we also obtain the (longitudinal) Thouless conductance g [35]. Both the typical and average

g decay exponentially with L_x, as is expected for localized one-dimensional systems. Interestingly though, we find that the *average* g retains a memory of the 2D critical scaling.

Existing studies of one-dimensional scaling of the integer quantum Hall problem [36,37] focus on open boundary conditions, where the crossover is seen through mixing of topological edge states on opposite edges of the strip. Our edge-free torus geometry offers a different perspective on the problem and reveals fascinating and unexpected behavior. Guided by these surprising numerical findings, we develop a theoretical understanding based on a mapping to a disordered Thouless pump [38] and clarify the meaning of the Chern number in the 1D limit. A quantitative description of the proliferation of Chern states follows naturally from this perspective.

Model and numerical method.—We consider a continuum model of two-dimensional (2D) electrons in a high perpendicular magnetic field such that the dynamics can be projected onto the LLL. The model is set on a rectangular torus with sides L_x, L_y such that $L_xL_y = 2\pi N_\phi \ell_B^2$, where $\ell_B = \sqrt{eB/\hbar}$ is the magnetic length, which we set to 1 henceforth. We define the aspect ratio $a = L_x/L_y$ and take $a \geq 1$. Disorder in the system is modeled by a Gaussian white noise potential $V(\mathbf{r})$, $\langle V(\mathbf{r}_1)V(\mathbf{r}_2)\rangle = U^2\delta^2(\mathbf{r}_1 - \mathbf{r}_2)$. We set $U = 1$ henceforth as disorder is the only energy scale in the problem: kinetic energy is quenched in the LLL; the cyclotron gap and interaction strength are taken to be infinite and zero, respectively. The torus has generalized periodic boundary conditions with angles $\boldsymbol{\theta}_{x,y}$. These also represent magnetic fluxes through the two nontrivial loops in the torus and are needed to define and compute Chern numbers of individual eigenstates in the disordered problem. For each disorder realization, we compute and diagonalize the single-particle Hamiltonian on a lattice of boundary angles $\boldsymbol{\theta}$ and store the eigenvalues $\{E_n(\boldsymbol{\theta})\}$ and eigenvectors $\{|\psi_n(\boldsymbol{\theta})\rangle\}$. The energies are used to calculate the Thouless conductance $g_n \equiv \mathbb{E}_{\theta_y}[\sigma_{\theta_x} E_n(\boldsymbol{\theta})]$ ($\mathbb{E}$ denotes averaging, σ denotes standard deviation), a measure of sensitivity to boundary conditions in the *long* direction; the wave functions are used to compute each eigenstate's Chern number C_n via a standard numerical technique [39]. Further details on the model and the numerical method are provided in the Supplemental Material [40].

Density of Chern states.—With the method outlined above, we calculate the density of states with Chern number C, $\{\rho_C(E) : C \in \mathbb{Z}\}$. These obey $\sum_C \rho_C = \rho$ (total density of states) as well as $\sum_C C\rho_C = \partial_E \sigma_{xy}$ (Hall conductance). Past studies [11,19] have characterized the 2D critical behavior by looking at the density of "current-carrying states," $\rho_{\text{top}}(E) \equiv \rho(E) - \rho_0(E)$. The width of ρ_{top} scales as $N_\phi^{-1/2\nu_{2D}}$ in the 2D thermodynamic limit.

In the present context, we observe completely different behavior. Namely, the width of ρ_{top} does *not* vanish as L_x is increased. It stays roughly constant for $a \gtrsim 1$, and

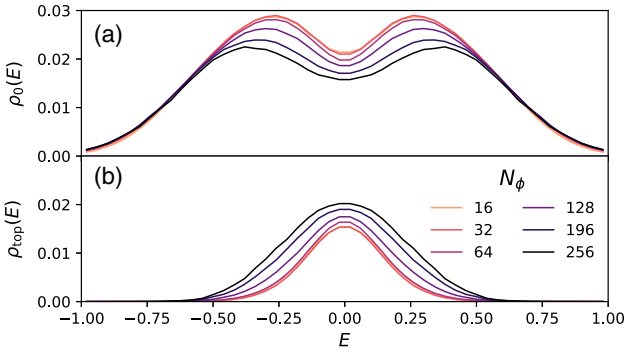

FIG. 1. Density of (a) $C = 0$ and (b) $C \neq 0$ states for fixed $L_y = 10$ and increasing N_ϕ. The density of Chern $C \neq 0$ states $\rho_{\text{top}}(E)$ grows and broadens at the expense of $\rho_0(E)$.

eventually starts *increasing* for $a \gg 1$ (Fig. 1). This increase is due both to the broadening of $\rho_{\pm 1}(E)$ (i.e., more pairs of Chern ± 1 states appearing away from the band center), and to an increase in higher-$|C|$ states. Despite these effects, the Hall conductance remains unchanged, and is determined by the shortest side of the torus [40]. It is as if percolating in *either* direction is enough for a state to acquire a nonzero Chern number.

This extensive number of topological current-carrying states seems to be incompatible with the localized nature of the spectrum (which we verify independently by means of the Thouless conductance and localization length). Reconciling these facts requires a careful analysis of the fate of Chern numbers as the dimensionality is tuned from $d = 2$ to $d = 1$ by increasing the aspect ratio a.

Thin-torus limit.—The above question is best addressed in the thin-torus limit $L_y \ll 1$, though (as we shall clarify later) the answer we find also applies to finite L_y, provided a is sufficiently large. The LLL Hamiltonian in the thin-torus limit is approximated by

$$H_{1D} = \sum_n v_n c_n^\dagger c_n + (t_n c_{n+1}^\dagger c_n + \text{H.c.}), \tag{1}$$

with $v_n = V_0(x_n)$, $t_n = e^{i\theta_x/N_\phi} V_1(x_n)$, and $x_n = (2\pi n + \theta_y)/L_y$. The V_m are partial Fourier transforms of the LLL-projected real-space disordered potential, $\tilde{V}(x, y)$, given by

$$V_m(x) \equiv \int_0^{L_y} \frac{dy}{L_y} e^{2\pi i m y/L_y} \tilde{V}(x, y). \tag{2}$$

LLL projection suppresses nonzero wave vectors, giving $t/v \sim e^{-\pi^2/L_y^2} \ll 1$. Further-neighbor hopping terms in Eq. (1) are exponentially smaller than t and can be neglected. In the following, we take $t_n \equiv te^{i\theta_x/N_\phi}$ for simplicity, as the precise magnitudes are unimportant. The angles $\boldsymbol{\theta}$ assume very different roles in this asymmetric limit: θ_x is the magnetic flux through the ring, while θ_y is the parameter of a Thouless pump [38] which smoothly

moves the Landau orbits relative to the background potential. At any fixed $\boldsymbol{\theta}$, the Hamiltonian of Eq. (1) is Anderson localized. As the pump parameter θ_y is adiabatically taken through a cycle, the random on-site potentials $v_n(\theta_y)$ change smoothly and the system undergoes spectral flow: at the end of the cycle, $v_n(2\pi) = v_{n+1}(0)$, so the initial and final spectra coincide up to a $n \mapsto n+1$ translation. However, following each eigenstate through the adiabatic cycle reveals an interesting picture.

Adiabatically changing a local chemical potential in an Anderson insulator leads to nonlocal charge transport [41] due to avoided resonances between the manipulated site and arbitrarily distant ones (the distance is practically limited by $\log\tau$, where τ is the timescale of the adiabatic manipulation; for calculating C, we can take $\tau \to \infty$). In the present setting, varying θ_y adiabatically manipulates all random fields at once, giving rise to a complicated network of resonances and thus more intricate patterns of charge transfer across the system. However, as a consequence of adiabaticity, an electron that starts the cycle in orbital n ends in orbital $n-1$ (i.e., at the same point in real space). Whenever two sites n_1 and n_2 are tuned past a resonance, charge is transported by a sequence of virtual nearest-neighbor hops through the shortest path between them [40]. One may expect each electron to take a local random walk in the vicinity of its initial site n_i before ending the cycle at site $n_i - 1$. However, this cannot be the case for every electron: at least one must wind around the entire system. Simple algebra shows that the winding numbers W_n of the electrons' paths must satisfy $\sum_n W_n = 1$ [40].

This bears intriguing similarity to the total Chern number of states in the Landau level, $\sum_n C_n = 1$. In fact, such an identification is correct: the Chern number C_n reduces to the winding number W_n in the thin-torus limit. This can be seen by considering the phase acquired during a loop around the "Brillouin zone" defined by $\boldsymbol{\theta}$. Threading flux θ_x does nothing to an Anderson localized wave function, whereas threading a quantum of θ_y flux causes it to wind W_n times around the ring, which encircles the θ_x flux. The net phase acquired is thus $2\pi W_n$, giving $C_n = W_n$. This can be straightforwardly made rigorous by partitioning the $\boldsymbol{\theta}$ torus into thin rectangular strips, so phases are defined unambiguously [40]. This identification is the key to explaining the observed proliferation of Chern states under 1D scaling. In essence, during a Thouless pump cycle, every electron hops randomly and nonlocally across the chain many times, generically acquiring a large winding number, and thus a large Chern number. Quantitatively, we find the number of steps in the random walk N_r diverges as $N_r \sim L_x$; the distribution of Chern numbers is approximately normal, with standard deviation $\sim L_x^{1/2}$ [40].

Dimensional crossover.—Even though the thin-torus limit $L_y \ll 1$ is a helpful simplification, the physics described above remains valid for $L_y > 1$, as long as $a \gg 1$. Hopping matrix elements are significant up to a real-space distance $\mathcal{O}(1)$, i.e., a number of sites $\mathcal{O}(L_y)$. These matrix elements are responsible for local level repulsion and strongly suppress energy fluctuations during the Thouless pump cycle. On a square torus, we know from numerics that the average Thouless conductance obeys $g(E,L) \simeq G(EL^{1/\nu_{2D}})$, where $G(x) \simeq g_0 e^{-x^2/2\sigma^2}$ is a scaling function and g_0 and σ are $\mathcal{O}(1)$ constants. Inverting the definition of g yields an estimate of the energy fluctuation δE of a typical state during the pump cycle:

$$\delta E \sim \frac{2\pi v g_0}{L^2} \exp\left(-\frac{E^2}{2\sigma^2} L^{2/\nu_{2D}}\right). \tag{3}$$

Here v is the bandwidth and $2\pi v/L^2$ is the typical level spacing. As δE is determined by the range of local hopping matrix elements, Eq. (3) remains true if we consider a rectangular torus and replace L with the *short* circumference L_y. The expected number of resonances encountered during a pump cycle, N_r, is proportional to the number of states in the spectrum with energies within the range of fluctuations δE. Approximating $\rho(E) \simeq (L_x L_y/2\pi v) e^{-\frac{1}{2}(E/\sigma')^2}$ (the exact expression [42] deviates slightly from a Gaussian) yields

$$N_r \sim \rho(E)\delta E \sim g_0 a e^{-\frac{1}{2}(E/E_0)^2}, \tag{4}$$

where E_0 is an L_x-independent energy scale. Thus, even away from the band center, and even for $L_y > 1$, increasing a eventually leads to $N_r \gtrsim 1$. At that point the crossover between 2D and 1D behavior takes place, with typical states acquiring a nontrivial winding number, equivalent to a nontrivial Chern number. This crossover happens unevenly in energy: it starts at the band center (where one already has Chern states even in the 2D thermodynamic limit) and spreads towards the band edges. The contour defining the crossover (fixed by setting $N_r \simeq 1$) is

$$E \sim \sqrt{\ln(a)}. \tag{5}$$

This prediction is borne out by numerical data on the density of Chern states, $\rho_C(E)$. Figure 2 shows that the broadening of ρ_{top}, already visible in Fig. 1, is explained fairly accurately as a scaling collapse of $\rho_C[E/\sqrt{\ln(a)}]$, for large enough a.

Thouless conductance.—As mentioned earlier, while 1D scaling causes the proliferation of Chern states across the spectrum, it also removes the critical energy characteristic of the 2D problem and makes the entire spectrum Anderson localized. We verify this numerically by calculating the disorder- and eigenstate-averaged Thouless conductance $g_{\text{av}}(E)$, Fig. 3(a). Unlike the 2D case, where at the center of the band $g_{\text{av}}(0) \sim \mathcal{O}(1)$ as $L \to \infty$, here we have $g_{\text{av}}(0) \sim e^{-L_x/\xi_1}$, as expected for a 1D problem (we find $\xi_1 \simeq 1.7 L_y$). However, surprisingly, the normalized

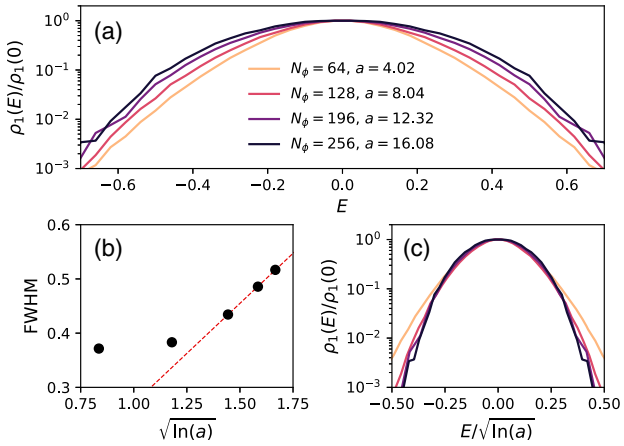

FIG. 2. (a) Density of $C = 1$ states $\rho_1(E)$ for $L_y = 10$ and varying aspect ratio a. (b) Full width at half maximum of ρ_1 indicates broadening consistent with Eq. (5). (c) Rescaling the energy by $\sqrt{\ln(a)}$ collapses the curves for different sizes.

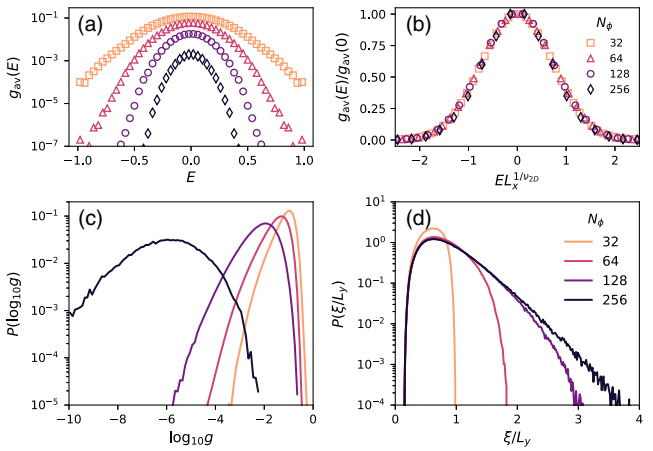

FIG. 3. (a) The average Thouless conductance $g_{av}(E)$ for $L_y = 14$ decays with increasing N_ϕ. (b) The normalized quantity $g_{av}(E)/g_{av}(0)$ shows scaling collapse under $E \mapsto EL_x^{1/\nu_{2D}}$ with critical exponent $\nu_{2D} \simeq 2.4$. (c) Distribution of $\log_{10} g(0)$ for $L_y = 10$, increasing N_ϕ. (d) Distribution of localization length ξ for the same system sizes. An exponential tail $P \sim e^{-c\xi/L_y}$ develops as N_ϕ increases.

quantity $g_{av}(E)/g_{av}(0)$ displays scaling collapse with the *same* critical exponent as the two-dimensional case, $\nu_{2D} \sim 2.4$ [43], Fig. 3(b). These results seem contradictory: on the one hand, a finite ξ_1 suggests localization across the spectrum with no critical energy; on the other, we observe signatures of a divergent $\xi_2 \sim E^{-\nu_{2D}}$, reproducing the 2D critical behavior, even as the scaling is purely one-dimensional.

The variation of g across samples and eigenstates sheds light on this issue. At the center of the band, the distribution of g broadens as L_x is increased and becomes approximately log-normal [the distribution $P(\ln g)$ is shown in Fig. 3(c)]. States in the positive tail of the distribution, which are abnormally extended in the *long* direction, dominate the average g_{av}. The appearance of ν_{2D} is to be expected as a consequence of such states: as they percolate across the sample in L_x but not in L_y, they are unaware of the aspect ratio, and thus display the 2D critical behavior. However, they are exponentially rare, which explains the vanishing amplitude of the signal and its presence in g_{av} but not g_{typ}. An exponential tail in the distribution of electron localization lengths $P(\xi/L_y)$ can be seen in Fig. 3(d); details on the definition and calculation of ξ, as well as additional data, are provided in Ref. [40].

Discussion.—We have investigated the fate of the quantum Hall plateau transition when the thermodynamic limit is taken in one dimension only. Through numerical diagonalization, we have uncovered surprising and counterintuitive behavior: Anderson localization across the spectrum, accompanied by the proliferation of Chern states. This led us to investigate the fate of the Chern number, a two-dimensional topological invariant, in the quasi-one-dimensional limit defined by $a = L_x/L_y \gg 1$. In the thin-torus limit $L_y \ll 1$, the system maps onto a 1D Anderson model with a Thouless pump parameter that smoothly shifts the random chemical potentials. During a pump cycle, electrons follow a random walk between resonant orbitals on the chain. We have shown that winding number W of the random walk around the system equals the Chern number C of the associated electron wave function. This identification leads to some striking predictions, e.g., that generic states in this limit have large, random Chern number.

We have further shown that the above picture is valid away from the thin-torus limit, i.e., for $L_y > 1$, as long as the torus aspect ratio a is large enough. The crossover between 2D and 1D behavior as a is increased starts at the band center and spreads towards the band edges. The broadening is predicted to be extremely slow, $\sim\sqrt{\ln(a)}$, but it is nonetheless visible in our numerics at $L_y \sim \mathcal{O}(10)$, quite far from the thin-torus limit.

On a theoretical level, our findings provide a new example of subtle interplay between topology and disorder [44–49]. The idea of topological pumping, which goes back to Thouless [38], is a subject of rising theoretical interest, especially in connection to Floquet physics [50–53] and synthetic dimensions [54]. Here it is applied in a new, disordered context, where it provides the key to interpret the quasi-1D limit of the quantum Hall plateau transition.

We conclude with some remarks related to experiment. As the nonlocal avoided crossings that underpin the picture presented here are generally very narrow (exponentially in system size), the adiabatic timescales required to observe this behavior in macroscopic systems are unphysically long. However, for microscopic systems, the manipulations required may still be performed adiabatically. The necessary

ingredients for a quantum simulation of this problem are (i) adiabatically tunable, pseudorandom on-site chemical potentials, (ii) nearest-neighbor hopping, and (iii) sufficiently long coherence times (relative to the required adiabatic timescale). Clean Thouless pumps have been successfully engineered using ultracold bosonic [55,56] or fermionic [57] atoms in optical superlattices, single spins in diamond [58], Bose-Einstein condensates [59], and quantum dots [60,61]; adding disorder could be an interesting new direction for these and other experimental platforms. Finally, while implementing periodic boundary conditions (i.e., arranging the qubits on a circle) in some such platforms may be problematic, the striking coexistence of Anderson localization and nonlocal charge transport across the length of the one-dimensional quantum simulator would be observable even on an open line segment.

This work was supported by DOE BES Grant No. DE-SC0002140. We acknowledge useful conversations with Shivaji Sondhi.

[1] K. v. Klitzing, G. Dorda, and M. Pepper, Phys. Rev. Lett. **45**, 494 (1980).
[2] R. B. Laughlin, Phys. Rev. B **23**, 5632 (1981).
[3] D. J. Thouless, M. Kohmoto, M. P. Nightingale, and M. den Nijs, Phys. Rev. Lett. **49**, 405 (1982).
[4] R. E. Prange, Phys. Rev. B **23**, 4802 (1981).
[5] B. Huckestein, Rev. Mod. Phys. **67**, 357 (1995), and references therein.
[6] H. P. Wei, D. C. Tsui, M. A. Paalanen, and A. M. M. Pruisken, Phys. Rev. Lett. **61**, 1294 (1988).
[7] L. W. Engel, D. Shahar, C. Kurdak, and D. C. Tsui, Phys. Rev. Lett. **71**, 2638 (1993).
[8] W. Li, C. L. Vicente, J. S. Xia, W. Pan, D. C. Tsui, L. N. Pfeiffer, and K. W. West, Phys. Rev. Lett. **102**, 216801 (2009).
[9] S. Kivelson, D.-H. Lee, and S.-C. Zhang, Phys. Rev. B **46**, 2223 (1992).
[10] I. A. Gruzberg, A. Klümper, W. Nuding, and A. Sedrakyan, Phys. Rev. B **95**, 125414 (2017).
[11] Q. Zhu, P. Wu, R. N. Bhatt, and X. Wan, Phys. Rev. B **99**, 024205 (2019).
[12] M. Puschmann, P. Cain, M. Schreiber, and T. Vojta, Phys. Rev. B **99**, 121301(R) (2019).
[13] B. Huckestein and B. Kramer, Phys. Rev. Lett. **64**, 1437 (1990).
[14] B. Huckestein, Europhys. Lett. **20**, 451 (1992).
[15] J. T. Chalker and P. D. Coddington, J. Phys. C **21**, 2665 (1988).
[16] D.-H. Lee, Z. Wang, and S. Kivelson, Phys. Rev. Lett. **70**, 4130 (1993).
[17] K. Slevin and T. Ohtsuki, Phys. Rev. B **80**, 041304(R) (2009).
[18] H. Obuse, I. A. Gruzberg, and F. Evers, Phys. Rev. Lett. **109**, 206804 (2012).
[19] Y. Huo and R. N. Bhatt, Phys. Rev. Lett. **68**, 1375 (1992).
[20] D. P. Arovas, R. N. Bhatt, F. D. M. Haldane, P. B. Littlewood, and R. Rammal, Phys. Rev. Lett. **60**, 619 (1988).
[21] K. Yang and R. N. Bhatt, Phys. Rev. Lett. **76**, 1316 (1996).
[22] K. Yang and R. N. Bhatt, Phys. Rev. B **55**, R1922 (1997).
[23] K. Yang and R. N. Bhatt, Phys. Rev. B **59**, 8144 (1999).
[24] D. N. Sheng and Z. Y. Weng, Phys. Rev. Lett. **75**, 2388 (1995).
[25] D. N. Sheng and Z. Y. Weng, Phys. Rev. Lett. **78**, 318 (1997).
[26] D. N. Sheng, X. Wan, E. H. Rezayi, K. Yang, R. N. Bhatt, and F. D. M. Haldane, Phys. Rev. Lett. **90**, 256802 (2003).
[27] X. Wan, D. N. Sheng, E. H. Rezayi, K. Yang, R. N. Bhatt, and F. D. M. Haldane, Phys. Rev. B **72**, 075325 (2005).
[28] R. N. Bhatt, Numerical approaches to the integer quantum Hall effect, in *Physical Phenomena at High Magnetic Fields: Proceedings of the National High Magnetic Field Laboratory Conference, Tallahassee, Florida*, edited by E. Manousakis (Addison-Wesley, Reading, 1992), p. 65.
[29] M. Ippoliti, S. D. Geraedts, and R. N. Bhatt, Phys. Rev. B **97**, 014205 (2018).
[30] J. Priest, S. P. Lim, and D. N. Sheng, Phys. Rev. B **89**, 165422 (2014).
[31] X. Wang, Q. Li, and C. M. Soukoulis, Phys. Rev. B **58**, 3576 (1998).
[32] N. Sandler, H. R. Maei, and J. Kondev, Phys. Rev. B **70**, 045309 (2004).
[33] P. W. Anderson, Phys. Rev. **109**, 1492 (1958).
[34] E. Abrahams, P. W. Anderson, D. C. Licciardello, and T. V. Ramakrishnan, Phys. Rev. Lett. **42**, 673 (1979).
[35] D. Thouless, Phys. Rep. **13**, 93 (1974).
[36] S. Kettemann, Phys. Rev. B **69**, 035339 (2004).
[37] A. Struck, B. Kramer, T. Ohtsuki, and S. Kettemann, Phys. Rev. B **72**, 035339 (2005).
[38] D. J. Thouless, Phys. Rev. B **27**, 6083 (1983).
[39] T. Fukui, Y. Hatsugai, and H. Suzuki, J. Phys. Soc. Jpn. **74**, 1674 (2005).
[40] See Supplemental Material at http://link.aps.org/supplemental/10.1103/PhysRevLett.124.086602 for details on the numerical calculations, a proof of the identity between Chern number and winding number, properties of the electrons' random walks, and additional data on the density of Chern states and electron localization length.
[41] V. Khemani, R. Nandkishore, and S. L. Sondhi, Nat. Phys. **11**, 560 (2015).
[42] F. Z. Wegner, Physik B **51**, 279 (1983).
[43] Such collapse is not seen for typical g.
[44] E. Prodan, T. L. Hughes, and B. A. Bernevig, Phys. Rev. Lett. **105**, 115501 (2010).
[45] D. A. Huse, R. Nandkishore, V. Oganesyan, A. Pal, and S. L. Sondhi, Phys. Rev. B **88**, 014206 (2013).
[46] B. Bauer and C. Nayak, J. Stat. Mech. (2013) P09005.
[47] Y. Bahri, R. Vosk, E. Altman, and A. Vishwanath, Nat. Commun. **6**, 7341 (2015).
[48] S. A. Parameswaran and R. Vasseur, Rep. Prog. Phys. **81**, 082501 (2018).
[49] Y. Kuno, Phys. Rev. B **100**, 054108 (2019).
[50] I. Martin, G. Refael, and B. Halperin, Phys. Rev. X **7**, 041008 (2017).
[51] P. Weinberg, M. Bukov, L. D'Alessio, A. Polkovnikov, S. Vajna, and M. Kolodrubetz, Phys. Rep. **688**, 1 (2017).
[52] M. H. Kolodrubetz, F. Nathan, S. Gazit, T. Morimoto, and J. E. Moore, Phys. Rev. Lett. **120**, 150601 (2018).

[53] A. Friedman, S. Gopalakrishnan, and R. Vasseur, Phys. Rev. Lett. **123**, 170603 (2019).
[54] I. Petrides, H. M. Price, and O. Zilberberg, Phys. Rev. B **98**, 125431 (2018).
[55] M. Lohse, C. Schweizer, O. Zilberberg, M. Aidelsburger, and I. Bloch, Nat. Phys. **12**, 350 (2016).
[56] M. Lohse, C. Schweizer, H. M. Price, O. Zilberberg, and I. Bloch, Nature (London) **553**, 55 (2018).
[57] S. Nakajima, T. Tomita, S. Taie, T. Ichinose, H. Ozawa, L. Wang, M. Troyer, and Y. Takahashi, Nat. Phys. **12**, 296 (2016).
[58] W. Ma, L. Zhou, Q. Zhang, M. Li, C. Cheng, J. Geng, X. Rong, F. Shi, J. Gong, and J. Du, Phys. Rev. Lett. **120**, 120501 (2018).
[59] H.-I. Lu, M. Schemmer, L. M. Aycock, D. Genkina, S. Sugawa, and I. B. Spielman, Phys. Rev. Lett. **116**, 200402 (2016).
[60] M. Switkes, C. M. Marcus, K. Campman, and A. C. Gossard, Science **283**, 1905 (1999).
[61] M. R. Buitelaar, V. Kashcheyevs, P. J. Leek, V. I. Talyanskii, C. G. Smith, D. Anderson, G. A. C. Jones, J. Wei, and D. H. Cobden, Phys. Rev. Lett. **101**, 126803 (2008).